ANALYTICAL AND COMPUTATIONAL SIMULATIONS OF EXPERIMENTAL DETERMINATIONS OF LINEAR VISCOELASTIC CONSTITUTIVE RELATIONS[1]

Cristina E. Beldica and Harry H. Hilton

Aeronautical and Astronautical Engineering Department, National Center for Supercomputing Applications, Center for Simulation of Advanced Rockets, University of Illinois at Urbana-Champaign, 104 South Wright Street, Urbana, IL 61801-2935 USA

SUMMARY: This paper addresses two important phenomena associated with interpretation of experimental viscoelastic material property data and of direct application to composites. (1) The influences of distinct ramp loading functions and of the rise time to full load on experimental material characterizations are investigated analytically and through numerical simulations and their important contributions to accurate material characterization are evaluated. (2) It is further demonstrated that the determination of relaxation and/or creep functions from the same experimental data in real time is a preferable protocol as it avoids additional unnecessary errors introduced through numerical transform inversions.

KEYWORDS: constitutive viscoelastic relations, material property characterizations, relaxation/creep function interrelations, simulations of experiments, viscoelasticity

INTRODUCTION

Experimental determinations of viscoelastic material properties are fraught with multiple pitfalls, such as non-repeatable tests on the same specimen, large data scatter, long time creep and relaxation data gathering, decelerating time effects due to lower temperatures and moisture contents, ineffective Laplace transform (LT) and Fourier transform (FT) compliance determinations from moduli transforms, to mention only a few. An additional set of problems arise from the fact that in many instances, particularly in polymers and composites, at temperatures above 21° C (70° F) and with moisture contents above .1 %, creep and relaxation initiation takes place in relatively short times compared to the largest relaxation times (Fig. 1). This requires impositions of loading patterns at sufficiently fast enough rates to achieve steady state loading conditions long before the start of creep and relaxation. Slow loading rates will cause loads (stresses) to intercept modulus curves too late and result in erroneous and misleading determinations of instantaneous elastic moduli $E(0) = E_0$, relaxation functions $\phi(0) = \phi_0$ and/or creep functions $\psi(0) = \psi_0$ (Fig. 1). As a matter of fact, the literature is replete with reports of E_0 dependence on temperature, when because of too slow loading rates partially relaxed values of viscoelastic moduli (or relaxation/creep functions) were actually measured and reported as elastic moduli E_0.

Equally disturbing are attempts to determined within acceptable precision boundaries, compliance time functions from moduli or creep functions from relaxation functions and vice versa in the time plane based on approximate time modulus/compliance relations instead of in the LT or FT domains based on exact relations. While such attempts are usually "justified" on the basis of inabilities to perform accurate numerical LT or FT inversions from numerical experimental data, the source of large $(\sim 100\%)$ errors are discussed in detail in Beldica & Hilton

[1]This research is supported by NCSA DoD Grant No. DAHC94-96-C-0005, High Performance Computing Modernization Program (HPCMP) and by CSAR DoE Grant No. B341494, Accelerated Strategic Computing Initiative (ASCI).

(1999), which also includes a comprehensive FFT bibliography.) Numerous highly efficient and accurate methods are readily available and can be carried out on desk top computers and certainly on work stations as well as on massively parallel supercomputers. More importantly, however, it is also shown that the LT or FT inversion accuracy problem can be totally avoided by working directly with the experimental data in the time domain to determine both relaxation and creep functions (or moduli and compliances) from the same experimental data set. Additionally, the separate importance of subjecting test specimens to two simultaneous loadings in order to recover both shear and Young's moduli are also discussed (Deng & Knauss 1997, Ravi-Chandar 1998).

In this paper, the influence of proper loading functions (rates) and the effects of inertia during high rate loadings are analyzed and evaluated with the help of numerical simulations under quasi-static and dynamic simulated experimental conditions. Various representative loading functions are considered and their relative merits are compared in so far proper material characterization is concerned.

Since numerical values of material parameters are sought, meaningful experiments need to be devised which can be solved analytically with symbolic values for the as yet unknown material parameters. Two distinct problems arise which influence material property determinations, namely (A) how steady state loads are achieved and (B) the effects of dynamic contributions due to specimen inertia. Both of these are considered separately and their effects are evaluated .

Bland (1960) and Kolsky (1963) have presented analytical formulations of viscoelastic wave propagations. Experimental studies of high dynamic loadings rates by Powers *et al.* (1995) using a split Hopkinson pressure bar have demonstrated the ability to determine instantaneous material properties in isotropic materials as well as in composites.

Due to space limitations, only summary concepts are presented here and full analyses and references may be found in Beldica & Hilton (1999).

ANALYSIS

Since numerical values of material parameters are sought, meaningful experiments need to be devised which can be solved analytically with symbolic values for the as yet unknown material parameters. Two distinct problems arise which influence material property determinations, namely (A) how steady state loads are achieved and (B) the effects of dynamic contributions due to specimen inertia. Both of these will be considered separately and their effects will be evaluated.

Consider a "simple" 1-D tension or compression (without buckling) creep experiment. In a Cartesian coordinate system $x = x_i$ with $i = 1, 2, 3$ and x_1 the loaded direction. Whether or not shear is present at $x_1 = 0$ in the x_2-direction has no bearing on the loading function formulation, but, of courses, influences internal stress distributions.

The loading function is defined in three time domains as (Fig. 2)

$$F(t) = \begin{cases} 0 & t \le 0 \\ F_0 \, f(t) & 0 \le t \le t_1 \\ F_0 \, H(t - t_1) & t \ge t_1 \end{cases} \tag{1}$$

where F_0 is a constant and $f(t)$ is typically one of such representative functions as

$$f(t) = \begin{cases} H(t) & t_1 = 0 \quad \text{and} \quad t \ge 0 & \text{Case 1} \\ t \,/\, t_1 & 0 < t_1 << \tau_1 & \text{Case 2} \\ .5 \, [1 - \cos(\pi \, t \,/\, t_1)] & 0 < t_1 << \tau_1 & \text{Case 3} \end{cases} \tag{2}$$

where $H(t)$ is the Heaviside unit step function. While mathematically all three functions are attainable, the only physically "reasonable" function is the third one, although other similar variations are equally acceptable, as it defines a gradual load rise from 0 to unity with vanishing slopes at $t = 0$ and $t = t_1$.

The time t_1 necessary to achieve the constant load F_0 is dictated by the laboratory equipment used to induce loadings. While t_1 has no predetermined relation to t_0, the time when relaxation begins, i. e. the relaxation modulus $E(t_0) = E_0$ (the instantaneous elastic Young's modulus) and $E(t) < E_0$ for $t > t_0$, the determination of moduli values are strongly influenced by the relative position of t_o and t_1. (See Table 1.)

The stress-strain relations for a linear homogeneous viscoelastic material with constant temperature and moisture content are given by (Christensen 1982, Hilton 1964a, Hilton & Dong 1964b)

$$\sigma_{ij}(x,t) \;=\; \int_0^t E_{ijkl}(t-t')\,\epsilon_{kl}(x,t')\,dt' \;=\; \int_0^t \phi_{ijkl}(t-t')\,\frac{\partial \epsilon_{kl}(x,t')}{\partial t'}\,dt' \quad (0 \le t \le \infty) \tag{3}$$

$$\epsilon_{ij}(x,t) \;=\; \int_0^t J_{ijkl}(t-t')\,\sigma_{kl}(x,t')\,dt' \;=\; \int_0^t \psi_{ijkl}(t-t')\,\frac{\partial \sigma_{kl}(x,t')}{\partial t'}\,dt' \quad (0 \le t \le \infty) \tag{4}$$

where $E_{ijkl}, J_{ijkl}, \phi_{ijkl}$ and ψ_{ijkl} are respectively the anisotropic relaxation moduli, compliances and relaxation and creep functions. While for anisotropic viscoelastic materials, there may be as many as 21 distinct functions for each of these, in the isotropic case only any two moduli or compliances (Young's, shear, bulk) or relaxation or creep functions or one of these and Poisson's ratio are needed to completely describe any material response plus, of course, thermal strain functions for non-isothermal conditions. However, Hilton & Yi (1997) have shown that linear viscoelastic Poisson's ratios $\nu(t)$ under many conditions are not only time dependent, but also a function of load and load path thus rendering ν non-unique and inappropriate for general material characterization. Additionally, normal strain measurements in two different directions are extremely difficult to obtain in non-metallic materials. Consequently, it is necessary to independently obtain any two of the three moduli or their corresponding creep or relaxation functions.

Deng & Knauss (1997) have devised experiments and apparatus to successfully measure the temperature and frequency dependence of dynamic bulk compliances of polyvinyl acetates. Pointing (1912) in an early work measured the shortening of a steel wire while being twisted, thus obtaining both elastic shear and Young's moduli from a single experiment. Popelar *el al.* (1990), among others, conducted extensive stress relaxation experiments at constant strain rates for viscoelastic characterization of polyethylene and presented master relaxation curves for this material. Ravi-Chandar (1997) has reported experiments of simultaneous volume dilatations and torsion, which produces characterizations of viscoelastic bulk and shear moduli from the same data. This procedure alleviates some of the experimental data scatter problem ever present in viscoelastic materials and which is additionally severely amplified when normal and shear strains are measured separately on different test specimens.

For isotropic conditions, the material property functions are related to each other through their Laplace (LT) or Fourier transforms (FT) of Eqs. (3) and (4) as

$$\overline{E}(p) \;=\; \frac{1}{\overline{J}(p)} \;=\; p\,\overline{\phi}(p) \;=\; \frac{1}{p\,\overline{\psi}(p)} \;=\; \frac{3\,\overline{G}(p)}{1 \,+\, \overline{G}(p)/\overline{K}(p)} \;=\; \frac{3\,p\,\overline{\phi}_s(p)}{1 \,+\, \overline{\phi}_s(p)/\overline{\phi}_v(p)} \tag{5}$$

Similar relations apply to G and K, respectively the isotropic shear and bulk moduli.
Their FT can be obtained through the fundamental inter-relation - provided the LT and FT each exist

$$\mathcal{FT}\{f(t)\} \;=\; \overline{\overline{f}}(\omega) \;=\; \overline{f}(p)\Big|_{p=\imath\,\omega} \tag{6}$$

Through the use of mechanical models, such as the generalized Kelvin (GKM) and generalized Maxwell (GMM) models, it can be shown that material properties are expressible in terms of Prony series

$$\phi(t) \;=\; \phi_\infty \;+\; \sum_{n=1}^{N} \phi_n \, \exp(-t/\tau_n) \quad \text{and} \quad \psi(t) \;=\; \psi_0 \;+\; \sum_{n=1}^{N} \psi_n \left[1 \;-\; \exp(-t/\tau_n)\right] \tag{7}$$

where the ϕ_n, ψ_n, τ_n and N are material property parameters to be determined by creep experiments under consideration. Similar expressions for $\overline{E}(p)$ and $\overline{J}(p)$ are obtainable from Eqs. (5) and (7). The instantaneous elastic values are then given by

$$\phi(0) \;=\; \phi_0 \;=\; \phi_\infty + \sum_{n=1}^{N} \phi_n \;>\; \phi_\infty \quad \text{and} \quad \psi(\infty) \;=\; \psi_\infty \;=\; \sum_{n=0}^{N} \psi_n \;>\; \psi(0) \;=\; \psi_0 \tag{8}$$

where ϕ_∞ and ψ_∞ are the fully relaxed values attainable only in relatively long times (Fig. 1). Expressions similar to Eqs. (7) can be derived for bulk and shear relaxation and creep functions (Beldica & Hilton 1999).

In a quasi-static analysis, at significant distances away from the supported end of the bar where St. Venant's principle applies, the normal stresses $\sigma_{11}(t)$ for $x_1 \;>\; 0$ are essentially directly related to the end loads at $x_1 = 0$ & L as $\sigma_{11}(t) = F(t)/A$, where A is the cross sectional area of the specimen.

When creep or relaxation experiments are conducted to determine material properties, one prescribes either stresses or strains and measures the other one. For instance in creep experiments where the load is known, the integral in Eq. (4) can be solved analytically by expressing $\psi(t)$ in terms of Prony series of Eq.(7). This leads to a nonlinear algebraic system of equations in the relaxation times τ_n

$$\epsilon_{11}(t) \;=\; \sigma_{11}^0 \left[\psi_0 \, f(t) \;+\; \sum_{n=1}^{N} \frac{\psi_n}{\tau_n} \int_0^t f(t') \, \exp\left(-\frac{t-t'}{\tau_n}\right) \, dt'\right] \qquad \text{for } t < t_1$$

$$\epsilon_{11}(t) \;=\; \sigma_{11}^0 \left\{\psi_0 \;+\; \sum_{n=1}^{N} \left[1 \;-\; \exp\left(-\frac{t-t_1}{\tau_n}\right) \;+\; \frac{1}{\tau_n} \int_0^t f(t') \, \exp\left(-\frac{t-t'}{\tau_n}\right) \, dt'\right]\right\}$$

$$\text{for} \quad t \geq t_1 \tag{9}$$

where $\sigma_{11}^0 \;=\; F_0/A$ and the unknown values are N, ψ_0, ψ_n and τ_n for $n = 1$ to N. The value of N is determined by trial and error so that $\psi(t)$ satisfies Eq. (9) to a preassigned degree of accuracy.

Similarly, relaxation functions can be determined from the same experimental data by invoking Eq. (3). The measured strains collected in tabular form as variables of time can be recovered in the time domain as analytical expressions by the method of least squares. Considering the typical shape of strain curves for viscoelastic materials, a curve fit using Prony series is convenient

$$\epsilon_{11}(x_1, t) \;=\; \epsilon_0(x_1) \;+\; \sum_{m=1}^{M} A_m(x_1) \left[1 \;-\; \exp\left(-\frac{t}{\tau_m}\right)\right] \tag{10}$$

Replacing this relation and the expression for $\phi(t)$ given by Eq. (6) into Eq. (3) gives after integration an expression similar to Eq. (10) for the measured σ_{11} and for the unknown ϕ_n and τ_n. These allow ϕ_∞, ϕ_n and τ_n for $n = 1$ to N to be determined by least square method. This protocol eliminates the necessity of calculating ψ from ϕ (or vice versa) by imposing an extra layer of approximate fast LT or FT approximate numerical inversion schemes. This

Table 1 - Definitions of Characteristic Times

TIME	DEFINITION
t_0	beginning of relaxation when $1 - E(t)/E_0 \leq \widetilde{\epsilon}_0$ for $t \geq t_0$
t_1	end of rise time when $F(t) = F_0$ for $t \geq t_1$
t_2	$= L/c_0$ time when wave reaches $x_1 = L$ from $x_1 = 0$
t_R	fully relaxed time when $1 - E(t)/E_\infty \leq \widetilde{\epsilon}_\infty$ for $t \geq t_R$
	$t_1 < t_0 < t_R$ and $t_R \leq t_2$ or $t_R \geq t_2$ Note: t_0, t_1, t_2 and t_R are independent of each other and where $\widetilde{\epsilon}_0$ and $\widetilde{\epsilon}_\infty$ each are $\ll 1$

point will be amplified and discussed in detail in a subsequent section. Care must, of course, be exercised to use identical N and τ_n values for both ϕ and ψ determinations.

In order to simplify the determinations of the unknowns and to linearize Eq. (10), one can assume a set of characteristic values for τ_n, such as for instance $\tau_n = 10^n$. Such prescribed τ_n are not their proper physical values corresponding to real relaxation times. Nor do the ϕ_n or ψ_n coefficients thus obtained represent physical values including the possibility of some individual negative signs, unless the τ_n are adjusted by trial and error. However, since in general one is only interested in the entire function $\phi(t)$ or $\psi(t)$ and not its detailed individual parts, the present approach is ideally suited to determine relaxation and/or creep functions in *toto*. An identical procedure with the same experimental data can again be used to obtain creep and relaxation functions ϕ and ψ from Eqs. (3) or (4). The recent work by Bradshaw & Brinson (1997) presents a more inclusive approach for the determination of compliances or moduli, since it guarantees proper detailed coefficient values including their algebraic signs.

If shear is generated through torsion with the same force F (Ravi-Chandar 1997), then the torque $M_T(t) = eF(t)$ (where e is a moment arm) obeys the same time definitions as $F(t)$. The torque and strains (rotational angles) can be measured experimentally. Using identical analytical formulations to those above for normal stresses and strains above, one can find the shear relaxation and creep functions ϕ_s and ψ_s (Beldica & Hilton 1999). Bulk relaxation functions can then be calculated from Eq. (5) or through individual volumetric experiments.

Bland (1960) has analyzed the 1-D impact problem of an isotropic homogeneous viscoelastic bar taking into account inertia and wave effects. Such analyses and experiments are an excellent vehicle for establishing correct values for the instantaneous elastic modulus E_0, since the latter is directly related to the readily measurable propagation velocity of the viscoelastic wave.

When considering dynamic behavior, an additional time parameter comes into play, namely t_2 the time for longitudinal waves to travel from their point of origin at $x_1 = 0$ to $x_1 = L$ and be reflected. The wave speed c_0 is elastic, however the end force is applied and whatever the linear viscoelastic properties $E(t)$ might be provided only that they exhibit instantaneous linear elastic responses. Under such conditions it is given by $t_2 = L/c_o = L\sqrt{\rho/E_o}$, with ρ the density of the viscoelastic material. (See Table 1 for definitions of the various characteristic times.)

The governing PDE for the dynamic longitudinal displacement $u_1(x_1, t)$ in an isotropic homogeneous linear viscoelastic material is

$$\frac{\partial^2 u_1(x_1,t)}{\partial t^2} = c_0^2 \int_0^t \widetilde{E}(t-t') \, \frac{\partial^2 u_1(x_1,t')}{\partial x_1^2} \, dt' \quad x_1 \in (0,L) \quad t \in (0,\infty) \tag{11}$$

with $E(t) = E_0 \, \widetilde{E}(t)$ and $1 \leq \widetilde{E}(t) \leq E_\infty/E_0$. In the LT space this PDE reduces to

$$p^2\,\overline{u}_1(x_1,p) \;=\; c_0^2\,\overline{\overline{E}}(p)\,\frac{\partial^2\overline{u}_1(x_1,p)}{\partial x_1^2} \tag{12}$$

Bland (1960) analyzed a rod with an impact load of $-\widehat{I}_0\delta(t)$ at $x_1 = L$ with a free end at $x_1 = 0$ and obtained the solution

$$\sigma_{11}(x_1,t) \;=\; -\frac{\widehat{I}_0}{\pi}\,\Re\left\{\int_0^\infty \exp\left(\imath\,\omega\,\left[t - x_1\sqrt{\rho\,\overline{J}(\omega)}\right]\right)\,d\omega\right\} \tag{13}$$

where $\widehat{I}_0$ is amplitude of the impact force per unit area.

In order to evaluate dynamic contributions to material property determinations, it is necessary to formulate the analysis for the loading patterns of Eqs. (1) and (2). First, it must be noted that *Case 1*, the Heaviside step function, is not feasible under dynamic conditions because its instantaneous load deployment presents a contradiction when inertia is taken into account. In *Case 2*, the linear load buildup in time gives rise to discontinuous time derivatives and infinite accelerations at $t = 0$ and $t = t_1$ and, therefore, is not acceptable dynamically. *Case 3* provides a smooth load transition of $F(t)$ from 0 to F_0 with second derivatives of $\pm .5(\pi/t_1)^2$ at $t = 0$ and t_1 respectively and is, therefore, reasonable physically and acceptable mathematically, although other functions with similar time rise characteristics may also be defined.

The solution of Eqs. (11) and (12) before reflection takes place is

$$\overline{u}_1(x_1,p) \;=\; \overline{f}_u\left[p, x_1, c_0\overline{\overline{c}}(p)\right] \tag{14}$$

or

$$\overline{u}_1(x_1,p) \;=\; \overline{A}(p)\;\sinh\left[\overline{k}(p)\,x_1\right] \;+\; \overline{B}(p)\;\cosh\left[\overline{k}(p)\,x_1\right] \tag{15}$$

$$\text{with} \qquad \overline{k}(p) \;=\; \frac{p}{c_0\sqrt{\overline{\overline{E}}(p)}} \qquad \text{for} \qquad 0 \le t \le t_2 \qquad \text{and} \qquad 0 \le x_1 \le L$$

where the functions $\overline{f}_u$, $\overline{A}$ and $\overline{B}$ are determined from boundary conditions and where

$$\overline{c}(p) = \sqrt{\rho/\overline{E}(p)} = c_0\,\overline{\overline{c}}(p) \qquad c_0 = \sqrt{\rho/E_0} \qquad \overline{E}(p) \;=\; E_0\,\overline{\overline{E}}(p) \tag{16}$$

$$\overline{\overline{c}}(p) = \sqrt{1/\overline{\overline{E}}(p)} = \sqrt{\overline{\overline{J}}(p)} \qquad \text{with} \qquad 1 \le \overline{\overline{c}}(p) \le \sqrt{J_\infty/J_0} \tag{17}$$

The boundary conditions for Case 3 are

$$\sigma_{11}(0,t) \;=\; \begin{cases} .5\;\sigma_{11}^0\;\left[1\;-\cos\left(\pi\,t/t_1\right)\right] & 0 \le t \le t_1 \\ \\ \sigma_{11}^0\;H(t-t_1) & t \ge t_1 \end{cases} \tag{18}$$

$$u_1(L,t) \;=\; 0 \qquad 0 \le t \le \infty \tag{19}$$

The 1-D governing relations (11) and (12) have a viscoelastic dynamic solution in $t \ge t_1$ for the above BC in the form of

$$\overline{\sigma}_{11}(x_1,p) \;=\; \overline{E}(p)\,\overline{\epsilon}_{11}(x_1,p) \;=\; \overline{E}(p)\,\frac{\partial\overline{u}_1(x_1,p)}{\partial x_1} \;=\; p\,\overline{\phi}(p)\,\frac{\partial\overline{u}_1(x_1,p)}{\partial x_1} \;=\; \tag{20}$$

$$\left\{\underbrace{\frac{c_0^2\,\sigma_{11}^0\;\left[\overline{I}_1(p)\;+\;\overline{I}_2(p)\right]}{p^2}}_{\overline{A}(p)}\right\}\;\left\{\cosh\;\left[\overline{k}(p)\,x_1\right]\;\underbrace{-\;\tanh\;\left[\overline{k}(p)\,L\right]}_{\overline{B}(p)/\overline{A}(p)}\;\sinh\;\left[\overline{k}(p)\,x_1\right]\right\}$$

where the $\overline{I}_1$ and $\overline{I}_2$ represent the LT integrals from 0 to t_1 and t_1 to ∞. Note that the functions $\overline{k}$ and $\overline{E}$ contain the as yet unknown material parameters, thus making a numerical LT inversion of Eq. (20) impossible. Formally, it can be inverted analytically much more readily as a FT by making use of relation (6)

$$\sigma_{11}(x_1, t) \;=\; \frac{1}{\pi}\,\Re\left\{\int_0^\infty \overline{\sigma}_{11}(x_1, \omega)\;\exp\left(\imath\,\omega\,t\right)\,d\omega\right\} \tag{21}$$

The inversion (21) cannot be carried out analytically because of the complexity of Eq. (20), integration by the convolution theorem cannot also be performed without prior knowledge of material properties. However, the results of these dynamic experiments serve to determine uniquely and accurately the value of the elastic modulus E_o and to check material property values determined by quasi-static experiments. (For details see Beldica & Hilton 1999.)

NUMERICAL SIMULATIONS AND DISCUSSION OF RESULTS

Loading protocols and their relation to creep and relaxation functions are shown in Figs. 1 and 2. As discussed before, the loading pattern and especially the time needed for the load (stress) to reach steady state conditions is reflected on the accuracy with which the material characteristics are determined. To exemplify this, a creep function was assumed and the corresponding strain curves were determined for the load cases 1, 2 and 3. Next the reference characteristic curve was shifted to the left, as would happen with temperature and/or moisture content increase. Since load case 1 represents an ideal situation, the shift does not affect the shape of slope of the strain curve (Fig. 3). For cases 2 and 3 the strain curves are altered if the stresses intercept the modulus curves after the material has started creeping (Fig. 4). It is worth emphasizing that a given load rate can be qualified as too slow not by the value of t_1, but by the relative position of t_1 to the creep function.

The next set of graphs present the creep functions determined by solving Eq. (9) for a given load case and different values of the loading time t_1. For illustration purposes the strain curves were established assuming that the material characteristics are known. The results obtained following the proposed procedure were compared to this reference curve. Times t_1 were chosen here by evaluating the increase in $\psi(t_1)$ compared to ψ_0. Since the values t_1 are not significant on their own, they will be identified on the plots by the relative increase in $\psi(t_1)$ from ψ_0.

Figs. 5 and 6 represent creep curves obtained by assuming that the loading conforms to an ideal situation, i.e. by replacing $f(t) = H(t)$ in Eq. (9). If the strain values used when solving the system of equations correspond indeed to case 1, the creep curve is recovered with good accuracy (less than 0.5% error for $N = 33$ terms in Prony series). However, if a more realistic situation is considered (case 2 and 3), the material characteristics are determined with some error depending on t_1. In Fig. 5 the strains were obtained from load case 2 and all the points $t < t_1$ were left out of the computation. As expected, the largest deviation appears in the values of ψ_0. Almost identical results were obtained using strains corresponding to load case 3 (Fig. 6).

For the next set of computations, the Prony coefficients were determined by replacing $f(t) = t/t_1$ in Eq. (9). If all points on the strain curve are used for the computation (including $t < t_1$) then the creep curve is determined very accurately if the strain corresponds to the same loading situation (Fig. 7). If this is not the case the algorithm breaks. A more conservative approach in which only the points $t > t_1$ are taken into account produces good results not only for the correct loading case, but also for similar loading patterns (Figs. 8 and 9). It is important that the time t_1 used for the least square method is the same as the one encountered in the loading pattern. Overestimating t_1 will lead to larger values for $\psi(t)$ as shown in the limit in Fig. 9 where the strains were obtained from load case 1. As a note of caution, for loading rates that go well into the creep portion of the characteristic curve the linearized least square algorithm can lead to badly scaled or close to singular matrices. This can be circumvented by increasing the number of terms in the Prony series and adjusting the set of characteristic times τ_n. Fig. 10 is similar to 5 except for different loading simulations, but exhibiting similar patterns.

Figs. 11 and 12 depict the results of the time domain relaxation function determination from the above described creep data. As before the relative errors are not caused by the used protocols but are due to the long t_1 loading times.

CONCLUSIONS

It is shown that loading patterns distinctly affect the determination of viscoelastic material property parameters, leading to possible erroneous or misleading characterizations. It is further demonstrated that it is possible to determine relaxation and creep functions in the time domain from identical test data, thus eliminating the need for approximate or numerical Laplace transform inversions and their inherent inaccuracies, which affect exact characterization determinations.

REFERENCES

Beldica, C. E. and H. H. Hilton (1999) ”Analytical and computational simulations of experimental determinations of deterministic and random linear viscoelastic constitutive relations,” *Technical Report UILU ENG 99-0502*, University of Illinois at Urbana-Champaign.

Bland, D. R. (1960) *The Theory of Linear Viscoelasticity*. Pergamon Press, New York.

Bradshaw, R. D. and L. C. Brinson (1997) “A sign control method for fitting and interconverting material functions for linearly viscoelastic solids,” *Mechanics of Time-Dependent Materials* **1**:85–108.

Christensen, R. M. (1981) *Theory of Viscoelasticity - An Introduction, 2nd ed.* Academic Press, New York.

Deng, T. H. and W. R. Knauss (1997) “The temperature and frequency dependence of the bulk compliance of poly(vinyl acetate). A re-examination,” *Mechanics of Time Dependent Materials* **1**:33–49.

Hilton, H. H. (1964a) “An introduction to viscoelastic analysis,” *Engineering Design for Plastics* (E. Baer, ed.) 199–276. Reinhold Publishing Corp., New York.

Hilton, H. H. and S. B. Dong (1964b) “An analogy for anisotropic, nonhomogeneous linear viscoelasticity including thermal stresses,” *Development in Mechanics* 58–73. Pergamon Press, New York.

Hilton, H. H., J. Hsu and J. S. Kirby (1991) “Linear viscoelastic analysis with random material properties,” *Journal of Probabilistic Engineering Mechanics* **6**:57–69.

Hilton, H. H. and S. Yi (1998) “The significance of anisotropic viscoelastic Poisson ratio stress and time dependencies,” *International Journal of Solids and Structures* **35**:3081–3095.

Kolsky, H. (1963) *Stress Waves in Solids*. Dover Publ., New York.

Pointing, J. H. (1912) “On the changes in the dimensions of a steel wire when twisted and on the pressure of distortional waves in steel,” *Proceedings of the Royal Society* **A86**:534–561.

Popelar, C. F., C. H. Popelar and V. H. Kenner (1990) “Viscoelastic material characterization and modeling of polyethylene,” *Polymer Engineering and Science* **30**:577–586.

Powers, B. M., J. R. Vinson, I. W. Hall and R. F. Hubbard (1995) “High-strain rate mechanical properties of Cycom 5920/1583 cloth glass/epoxy composites,” *AIAA Journal* **35**:553–556.

Ravi-Chandar, K. (1998) “Simultaneous measurement of nonlinear bulk and shear relaxation behavior,” *Proceedings of the 2nd International Conference on Mechanics of Time Dependent Materials* 30–31. SEM, Ljubljana, Slovenia.

Schapery, R. A. (1962) “Approximate methods of transform inversion for viscoelastic stress analysis,” *Proceedings Fourth US National Congress of Applied Mechanics* **2**:1075–1085. ASME, New York.

Fig. 1 LOADING FUNCTIONS & RELAXATION FUNCTIONS

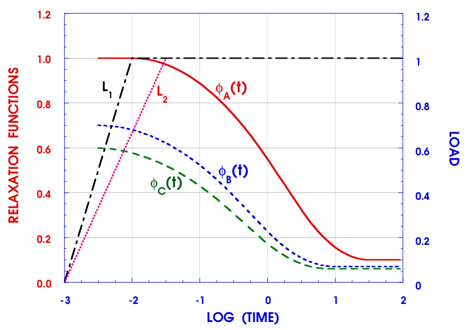

Fig. 2 TRUE AND APPARENT YOUNG'S MODULUS

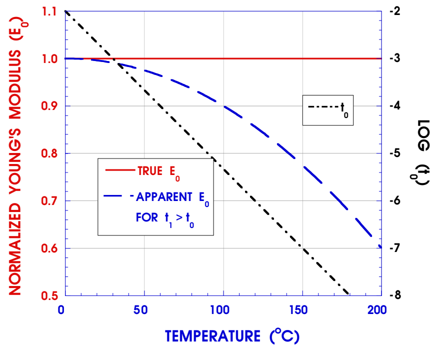

Fig. 3 RELAXATION FUNCTION TIME SHIFTS

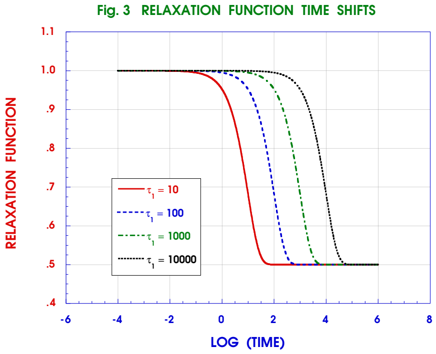

Fig. 4 TEST SPECIMEN

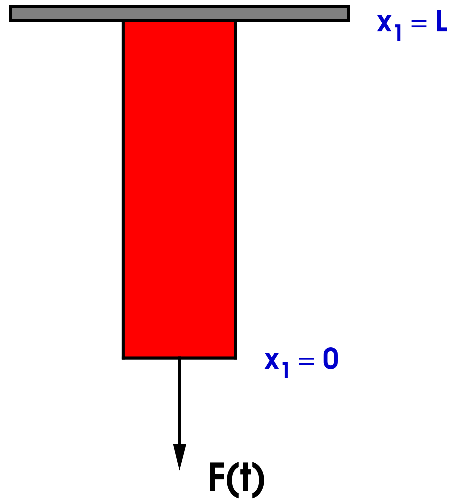

Fig. 5 LOAD RAM FUNCTIONS AND RELAXATION FUNCTION

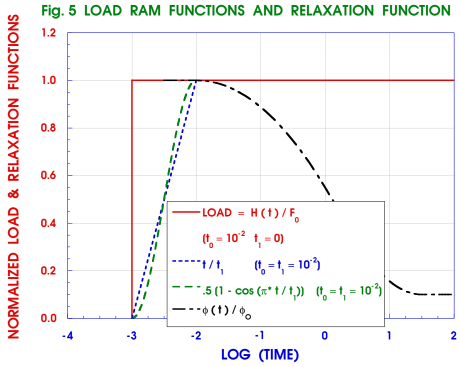

Fig. 6 LOADING RAM TIME VS. LARGEST RELAXATION TIME

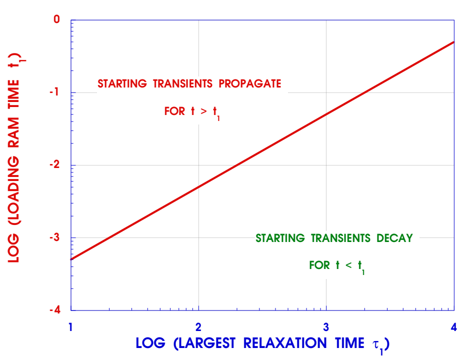

Fig. 7 J APPROXIMATION (E_∞=.2, E_1=.8, τ=100)

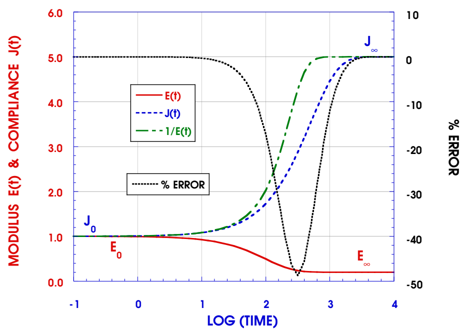

Fig. 8 PER CENT ERROR FOR J APPROXIMATION

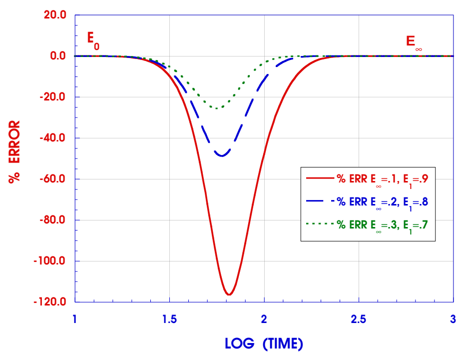

Fig. 9 MAXIMUM % ERROR FOR J APPROXIMATION

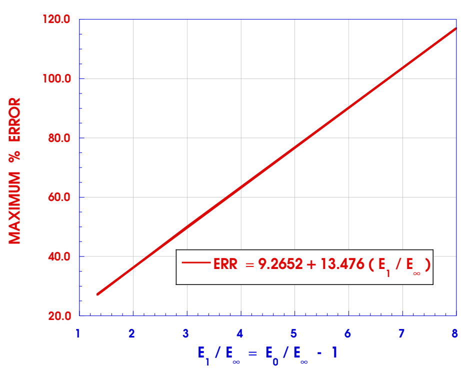

Fig. 10 STATISTICAL RELAXATION FUNCTION DISTRIBUTION

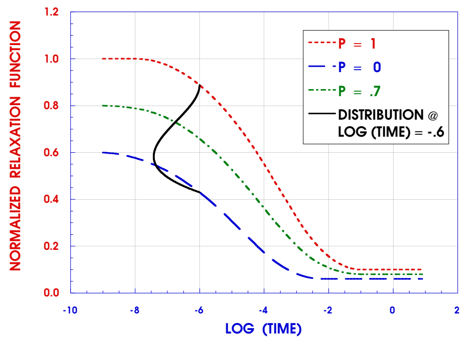

Fig. 11 LOAD CASE 1

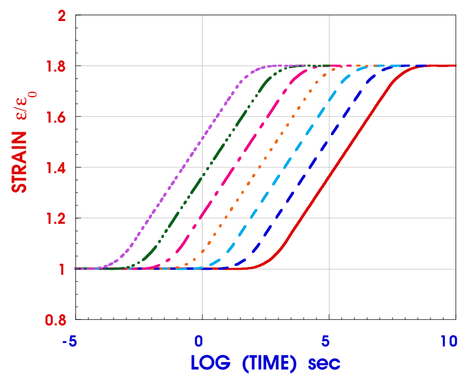

Fig. 12 LOAD CASE 2